

New insights into the modulation of ocean biogeochemistry by iron

Alessandro Tagliabue^{1*}, Andrew Bowie², Philip Boyd², Kristen Buck³, Kenneth Johnson⁴ and Mak Saito⁵

1. University of Liverpool, United Kingdom

2. Institute for Marine and Antarctic Studies, University of Tasmania, Australia

3. University of South Florida, USA

4. Monterey Bay Aquarium Research Institute, USA

5. Woods Hole Oceanographic Institution, USA

*Corresponding author: a.tagliabue@liverpool.ac.uk

Preface

Our understanding of the regulation of the magnitude of global and regional primary productivity has been fundamentally altered with the growing recognition of the pervasive role of iron.

Observations of this trace metal in the ocean have increased markedly over recent decades, permitting a new synthesis of the processes governing its oceanic cycle. In particular, the inextricable linkages between iron and wider ocean biogeochemistry, including the cycling of carbon and major nutrients are beginning to emerge.

1. The emergence of the ‘Iron Hypothesis’

Ocean primary production is crucial to the Earth System, underpinning the functioning of the global carbon cycle, air-sea CO₂ exchange and marine ecosystems¹. In the past three decades the micronutrient iron has gone from a relative curiosity to emerging as a key elemental resource that shapes the magnitude and dynamics of primary production in the global ocean. Oceanographers first became interested in iron in the 1930s as an explanation as to why the major nutrient inventories (nitrogen and phosphorus) were not fully depleted by primary producers in surface waters of much of the Southern Ocean²⁻⁴. Indeed, early laboratory studies showed that iron enrichment stimulated the growth of phytoplankton⁵, providing encouragement that iron could control phytoplankton growth in seawater^{6,7}. However, due to the low solubility of iron in the modern oxic ocean⁸ and the tendency for iron to be ‘scavenged’ from the water column by sinking particles⁹, dissolved iron was likely to be a rare commodity for ocean biota. By the early 1980s the crucial role for iron as a co-factor in many cellular enzymes, particularly those linked with photosynthesis, respiration and nitrogen fixation had been identified^{10,11}. Yet despite this body of knowledge, it was not until the early 2000s that the global importance of iron to ocean productivity and biogeochemistry became widely acknowledged and included in global ocean models¹².

A key issue hindering the study of iron-phytoplankton interactions in the ocean was the need for contamination-free sampling and accurate measurements at the required pico to nanomolar levels (10⁻¹² to 10⁻⁹ moles L⁻¹). Only in the late 1970s did development of exacting trace metal clean sampling protocols¹³ and an appreciation for the rigours of clean analytical methods¹⁴ allow the first reliable oceanic iron observations, which showed low surface water concentrations and ‘nutrient-like’ behaviour through the water column^{15,16}. Results from shipboard iron enrichment experiments of natural phytoplankton communities conducted with ultra-clean methods resurrected the idea that a lack of iron was indeed a key feature of the Southern Ocean^{17,18}. This led John Martin to formulate the ‘*iron hypothesis*’, which proposed that greater delivery of dust iron to the Southern Ocean during glacial periods led to enhanced utilisation of the major nutrients and a corresponding drawdown of atmospheric carbon dioxide¹⁹ (see also Box 1). Subsequent model simulations showed that if the reserves of major nutrients in the Southern Ocean could be exhausted, then atmospheric CO₂ levels could be reduced significantly by 60 to 100 ppm²⁰. Martin’s provocative ideas about how iron fertilisation might control past and future climate are now oceanographic folklore and have catalysed research into this field.

57 Due to the perceived limitations of Martin's shipboard experiments (e.g. exclusion of grazers)²¹,
58 only a deliberate *in situ* iron fertilisation was deemed able to satisfactorily corroborate the *in vitro*
59 evidence of iron-limited phytoplankton growth. These were initially performed during the 1990s in
60 iron-limited equatorial Pacific waters^{22,23} and by 2000, results were published from the first test of
61 the iron hypothesis in the Southern Ocean²⁴. As of present, more than a dozen mesoscale iron
62 fertilisation experiments have been carried out worldwide, demonstrating phytoplankton iron
63 limitation in the Southern, Equatorial Pacific and subarctic Pacific Oceans^{25,26}. Additional shipboard
64 experiments also point to a role for iron limitation in the subpolar North Atlantic Ocean²⁷, California
65 Current²⁸ and Humboldt and Peru upwelling systems²⁹.

66
67 The undeniable role for iron in shaping patterns of ocean productivity necessitated an
68 understanding of the processes that regulate the ocean iron cycle itself. In 1997 an important step
69 was made when Johnson and co-workers³⁰ compiled 354 internally consistent iron observations
70 and produced a conceptual view of how the ocean iron cycle operated (Fig. 1), which was
71 supported by a one dimensional model that reproduced observed profiles from a number of sites
72 (largely in the Pacific Ocean). This model³⁰ assumed that (i) iron-rich aeolian dust input was the
73 major external source of iron to the ocean, (ii) deep ocean iron concentrations were held to a
74 quasi-constant value of approximately 0.6 nmol L⁻¹ by uniform levels of the recently quantified
75 organic iron-complexing ligands^{31,32} that protected dissolved iron from scavenging and (iii) that
76 despite emerging knowledge of substantial variations in the biological iron demand³³, the uptake of
77 iron and its regeneration from sinking organic matter was closely coupled to phosphorus at basin
78 scales. This synthesis effort³⁰ (Fig 1) ultimately catalysed the full representation of iron cycling with
79 three dimensional ocean general circulation models^{34,35}. Subsequent synthesis efforts in the
80 following years^{36,37} echoed this general paradigm for the ocean iron cycle, which still informs a
81 large number of global iron models today³⁸. Models based on this view of the ocean iron cycle
82 attribute up to half of the 80 ppm glacial decrease in atmospheric carbon dioxide to iron
83 fertilisation^{39,40}.

84
85 In this Review we will explore how the recent expansion of observational data has challenged the
86 prevailing understanding of the ocean iron cycle. New sources and cycling processes are
87 identified, which requires an overhaul of the way in which the models we rely on for future
88 projections represent this important resource. These insights permit a new synthesis of the main
89 processes involved in the global ocean iron cycle and the important linkages to the cycling of
90 carbon and other nutrients. Ultimately we highlight where future advances may be fruitful in
91 advancing our understanding. If this can be achieved, it would substantially reduce uncertainties in
92 our ability to project the impact of environmental change on the ocean carbon cycle.

93 94 **2. Refining our understanding of the iron cycle and its biogeochemical linkages**

95
96 In recent years there has been a near 100-fold increase in the number of high quality iron
97 measurements available to explore processes and assess global models⁴¹. Initially, only a few
98 laboratories worldwide had the capability to sample for and measure iron in the ocean, resulting in
99 relatively sparse datasets. In an effort to remedy this, in the early 2000's the international
100 community galvanised around a global project called "GEOTRACES" (www.geotraces.org) that
101 seeks to systematically document the distribution of trace elements and isotopes, including iron,
102 throughout the oceans⁴². Critical in this regard was an earlier intercalibration effort in 2004 called
103 "Sampling and Analysis of Iron" (SAFe) that sought to intercompare a suite of analytical techniques
104 and trace metal clean sampling methodologies from different laboratories at sea⁴³. Importantly, it
105 also produced a set of readily available 'reference samples' with consensus values at
106 oceanographically relevant concentrations that could be used by both new and established
107 investigators to evaluate their analytical methods. GEOTRACES has since launched a number of
108 interwoven basin-scale "sectional" studies, complemented by prior targeted process studies to
109 understand temporal iron dynamics⁴⁴ and the drivers of "naturally fertilised" regions in the wake of
110 Southern Ocean island systems^{45,46}. Thanks to these multi-faceted efforts, there are more than
111 20,000 available observations of iron from the ocean at present. This expansion in our ability to
112 observe the system has allowed our understanding of how the ocean iron cycle operates to be
113 refined.

114
115
116
117
118
119
120
121
122
123
124
125
126
127
128
129
130
131
132
133
134
135
136
137
138
139
140
141
142
143
144
145
146
147
148
149
150
151
152
153
154
155
156
157
158
159
160
161
162
163
164
165
166
167
168
169
170

2.1 Recognition of external sources and cycling of iron

A key finding from both the GEOTRACES programme and studies of process studies of natural systems was the recognition that there are multiple external sources of iron to the ocean that are significant at both regional and global scales. For example, studies of enhanced biological activity downstream of Southern Ocean island systems^{45,46} and offshore from continental margins⁴⁷, the ability to track the origins of offshore iron pools via its mineral make up⁴⁸ and parallel modelling experiments⁴⁹ have emphasised that iron supply from continental margins extends far beyond the coastal zone. Equally, GEOTRACES efforts in the Atlantic⁵⁰, Pacific⁵¹, Southern⁵² and Arctic⁵³ Oceans have observed striking signals of iron associated with hydrothermal activity along mid ocean ridges that make a key contribution to the deep ocean iron inventory^{49,54}. Due to their important role in the high latitude regions of the ocean crucial for air-sea CO₂ exchange, continental margin and hydrothermal sources play a dominant role in shaping the global carbon cycle⁴⁹. However, the role for dust may have been enhanced during glacial periods typified by greater Southern Ocean dust fluxes.

While the perceived role for dust in regulating the functioning of the ocean carbon cycle via its modulation of high latitude ocean productivity has diminished in recent years, it remains a key supply mechanism to the low latitude ocean. This is illustrated by new high precision iron isotope studies that have, via the distinct isotopic signal associated with crustal iron, quantified the contribution of dust to dissolved iron in the tropical Atlantic Ocean⁵⁵. The productivity of this region is typically limited by nitrogen⁵⁶ and when enough iron is supplied it permits the growth of nitrogen-fixing organisms⁵⁷. More broadly speaking, iron supply has emerged as a major driving force behind the geographic extent and magnitude of nitrogen fixation in the tropics⁵⁸⁻⁶⁰. Dust-driven changes in iron supply to the low latitude ocean has therefore emerged as an important component of the maintenance of the oceanic fixed nitrogen inventory⁶¹.

An important hypothesis from the initial view of the ocean iron cycle was the concept of the buffering of dissolved iron to a constant deep-water concentration by uniform concentrations of organic iron-complexing ligands. However, a parallel expansion of ligand observations over recent decades^{62,63}, including basin scale ocean sections^{64,65}, reveals that their abundance varies from less than 1 to more than 2 nmol L⁻¹ even in the ocean interior. Potential ligand sources associated with iron-limited bacterial and phytoplankton community growth, zooplankton grazing and particle breakdown have emerged⁶², as well as potential external inputs associated with dust⁶⁶ or rainwater⁶⁷ and the microbial production of strong iron-binding siderophores⁶⁸. There is also the likelihood that subduction and equatorward transport of excess ligands from high latitudes can remotely influence the interior distribution of dissolved iron⁶⁹. As they control the residence time of iron in the ocean⁷⁰, the cycling of organic iron-complexing ligands has also emerged as a crucial component of the ocean iron cycle. For instance, modelling indicates that variations in ligand concentration have a larger influence on contemporary atmospheric carbon dioxide levels than dust iron supply⁴⁹ and can be responsible for long range transport of iron away from point sources (e.g. hydrothermal vents)⁵¹.

2.2 Biological Iron Cycling

The phytoplankton demand for iron relative to carbon or phosphorus (i.e. their 'stoichiometry') is a common way of evaluating the coupling between the biological cycling of different resources. Despite its initial representation in numerical and conceptual models (Fig 1) as a constant quantity^{30,35}, it is now well established that phytoplankton can exhibit substantial variations in their iron stoichiometry between different environments^{33,71}. For example, phytoplankton from the low iron waters of the Southern Ocean typically exhibit cellular demands that are more than five-fold lower than those from the iron rich tropical Atlantic^{71,72}. This level of stoichiometric plasticity extends far beyond that seen for the major nutrients⁷³ and is crucial in linking the biological cycling of iron to the assimilation of major nutrients and carbon fixation. Another unique feature for iron is the key role for iron regeneration by zooplankton, bacteria and viruses in supporting iron supply to the biota⁷⁴. A number of process studies have documented regional and seasonal variation in the

171 importance of regenerated iron in fuelling phytoplankton carbon fixation^{74,75} and a potentially
172 important role for higher trophic levels organisms is also emerging⁷⁶. Lastly, specific characteristics
173 associated with remineralisation of particulate iron, relative to major nutrients⁷⁷ can decouple the
174 vertical profile of dissolved iron in the ocean from other nutrients⁷⁸.

175
176 How iron affects rates of carbon and nitrogen fixation is fundamentally linked to the process of iron
177 acquisition by the biota. Early studies demonstrated that only the dissolved iron not bound to iron
178 complexing organic ligands was bioavailable^{6,79}. While the sum of these 'free' inorganic species
179 may indeed be the most bioavailable form of iron⁸⁰, its concentration in seawater is vanishingly low
180 ($<10^{-15}$ moles L^{-1}). More recently, laboratory⁸¹ and field⁸² experiments have demonstrated that
181 phytoplankton are also able to access the more dominant organically complexed iron pool via high
182 affinity acquisition systems, such as ferric reductases and this strategy appears to be prevalent in
183 the iron-poor Southern Ocean⁸¹. In the dust dominated low latitude regions of the Atlantic Ocean
184 the nitrogen fixing cyanobacterium *Trichodesmium* has been shown to directly access mineral
185 particulate iron⁸³. Taken together, this highlights a range of iron acquisition strategies that may be
186 differentially linked to the commonly measured 'dissolved' iron concentration.

187
188 When detailed process studies combine measurements of ocean physics, major nutrient
189 distributions and inputs with biological activity the intricate links between the cycling of iron and
190 other nutrients and carbon can be illuminated. Across the tropical Atlantic Ocean it has been
191 demonstrated that synoptic variation in dust input, linked to variations in the Inter Tropical
192 Convergence Zone, controls the 'biogeochemical divide' between phosphorus and iron limitation of
193 nitrogen fixing plankton⁵⁹. In the Pacific Ocean, metaproteomic techniques find gradual transitions
194 from nitrogen to iron stress between the subtropical Pacific Gyre and the Equatorial Pacific that are
195 linked to the underlying physics, with continuing iron stress in the south Pacific Gyre⁸⁴. These
196 approaches provide basin-scale perspectives on how the distinct environmental characteristics of
197 different ocean biomes translate into gradients in the resource regulation of biological activity.

198

199 **2.3 A new synthesis of the ocean iron cycle and its wider connections**

200

201 Bringing together these new insights allows an updated synthesis of how the ocean iron cycle
202 operates and its connections with the cycles of carbon and nitrogen (Fig 2). In doing so, we are
203 required to make a broad distinction between the dominance of dust iron at low latitudes and the
204 greater role for sedimentary and hydrothermal iron sources at high latitudes. While iron supply at
205 the high latitudes drives the connections to the wider oceanic cycling of carbon and air-sea carbon
206 dioxide exchanges, low latitude dust supply contributes to the maintenance of the fixed nitrogen
207 inventory of the ocean. The drivers of the interior distribution of iron are more complicated than for
208 major nutrients (see Box 1), with roles played by deep ocean iron sources, the independent
209 regeneration of iron from sinking particles and scavenging, as well as by the remote influence of
210 water masses subducted from high latitudes and transported equatorward. Previously, close
211 linkages between the cycling of iron and major nutrients such as phosphorus were emphasised
212 (Fig 1). However, as discussed above, multiple unique factors for iron have now been identified,
213 exemplified by the substantial decoupling between observations of phosphate and iron along a
214 meridional section in the West Atlantic Ocean⁸⁵ (Fig 3).

215

216 Synthesising these new insights provides a more refined picture of the ocean iron cycle and
217 emphasises key meridional contrasts (Fig 2). At high latitudes, upwelling and mixing of iron into
218 surface waters is the major supply mechanism fuelling biological activity that is sustained via iron
219 recycling by zooplankton and bacteria. Due to longer remineralisation length scales, iron export to
220 the ocean interior is more efficient than for major nutrients (phosphorus is emphasised in Fig 2)
221 and decouples subsurface iron reserves from those of major nutrients⁷⁸. As high latitudes are often
222 iron limited, ligand production by iron stressed communities and depletion of dissolved iron stocks
223 leaves an excess of iron-complexing ligands that can be subducted and transported equatorward
224 (dashed arrows in Fig 2). In contrast, low latitudes are strongly affected by dust and the associated
225 iron supply fuels nitrogen fixation by *Trichodesmium*, *Crocospheara* and other diazotrophs. Dust
226 may act as a source or sink for iron both in the surface ocean and during its sedimentation into the
227 ocean interior. For example, in the iron replete Mediterranean, dust deposition actually depleted

228 dissolved iron levels due to the enhanced particle scavenging⁸⁶. In low latitude regions where dust
229 supply is low and upwelling absent, the ensuing iron stress leads to low rates of nitrogen fixation⁸⁷.
230 Subsurface iron at low latitudes will be affected by the balance between local iron regeneration
231 from sinking organic material and scavenging onto lithogenic and organic particles⁸⁸. As
232 scavenging rates are closely linked to the amount of iron not organically complexed, subsurface
233 iron in the low latitudes can also be remotely controlled by subduction and equatorward transport
234 of high latitude waters with excess ligands⁶⁹.

235
236 This integrated view of the ocean iron cycle places additional challenges on the global ocean
237 models we rely on for testing hypotheses and projections of change. For example, those global
238 models that more closely track the developments in our understanding of the ocean iron cycle
239 encapsulated in Fig 2 are better able to reproduce observed features emerging from the iron data
240 collected along large GEOTRACES ocean sections³⁸. When models reflect the existence of
241 multiple iron sources and unique aspects to iron's oceanic cycling, simulated glacial iron
242 fertilisation contributes less than a quarter to decrease in the glacial carbon dioxide (despite
243 enhancing Southern Ocean biological activity)⁸⁹. At present, inter-model differences result in iron
244 residence times that range widely, from a few years to a few hundred years³⁸. This uncertainty
245 regarding the representation of iron in global models is important as projections of how climate
246 change will affect ocean productivity⁹⁰, which has implications for global carbon cycling and marine
247 ecosystems, will be regulated by iron over large swathes of the upper ocean. Reducing uncertainty
248 requires that we are able to dig deeper into the new oceanic survey data to extract quantitative
249 information on the rates and controlling factors of the mechanisms governing the ocean iron cycle
250 to inform accurate model parameterisations.

251

252 **3. Linking iron to the cycles of carbon and other nutrients: new challenges and** 253 **opportunities**

254

255 The rapid increase in iron observations over recent decades has led to a much clearer
256 understanding of the myriad processes underpinning the ocean iron cycle and its connections to
257 the cycling of carbon and major nutrients (Fig 2). However, a complete theoretical framework for
258 how iron cycling embeds within the broader context of ocean biogeochemical cycling is still lacking,
259 which limits our ability to project future trends with confidence³⁸. The expanding coverage of ocean
260 observations via the GEOTRACES surveys⁴¹ is essential, but alone is insufficient to constrain the
261 key underlying processes.

262

263 **3.1 Physical linkages across different space and time scales**

264

265 The new proliferation of full depth, basin scale ocean sections for iron have been instrumental in
266 advancing our understanding of the ocean iron cycle (Fig 2). However, the 'biogeochemical'
267 processes of interest (e.g. iron regeneration, scavenging, ligand production) operate on the
268 backdrop of different physical processes that must be taken into consideration to extract
269 information on the underlying biogeochemical processes (see Box 1). For instance, a given
270 oceanic section is overlain with signatures of different water masses reflecting their individual end
271 member conditions, interior flow pathways and transit times, which confound interpretation of iron
272 distributions. That said, observed features in iron distributions can themselves be 'fingerprinted'
273 using conservative tracers (either steady state or transient) of specific iron sources and cycling
274 pathways.

275

276 Water masses leave the ocean surface via the process of subduction and are transported along
277 lines of constant potential vorticity in the ocean interior⁹¹. Therefore, water masses provide a
278 framework for the deeper examination of biogeochemical properties. For example, on the recent
279 zonal GA03 GEOTRACES section in the North Atlantic Ocean, an Optimum Multi Parameter
280 Analysis was undertaken whereby the hydrographic and major nutrient data was used to
281 objectively identify nine primary watermasses⁹². Such a physical framework permits the evaluation
282 of how water masses originating from different locations, with specific iron characteristics (e.g. low
283 iron water from the high latitudes and high iron Mediterranean water) affect the distribution of iron
284 throughout the basin. The vertical distributions of iron at a given location should be evaluated in its

285 proper physical context (i.e. in density space), to account for the physical variability that often
286 complicates interpretations based on absolute depths⁷⁸.

287
288 Steady state and transient tracers provide an excellent opportunity to fingerprint specific iron
289 sources and assess iron input fluxes or regeneration and scavenging rates. Volcanic helium-3 has
290 been used to identify iron plumes associated with mid ocean ridges^{50,51,54}, as well as derive large
291 scale hydrothermal fluxes when estimates of global helium efflux are combined with the slope of
292 the iron versus helium relationship⁵¹. The radium decay series, which is used to quantify
293 exchanges at ocean boundaries, is also measured on some GEOTRACES sections⁹³ and may be
294 linked to dissolved iron datasets to estimate a range of iron boundary fluxes. A particularly
295 promising avenue may be the combination of such tracers with iron isotope studies. Tracers of
296 ocean ventilation, such as chlorofluorocarbons or tritium, and diagnostics of interior ocean flows,
297 such as potential vorticity, can be used to provide a coherent context within which to quantify how
298 iron concentrations are modified, e.g. by regeneration or scavenging, during the transit of a water
299 parcel subducted from the ocean surface (see: Box 1, Fig 4a) or away from a specific point source
300 (e.g. a mid ocean ridge or continental margin). As shown in Fig 3, phosphate distributions are
301 almost always closely linked to lines of constant potential vorticity following the major physical
302 flows, whereas the distributions of iron have little obvious connection, highlighting distinctions
303 between the cycling of these two nutrients.

304
305 Ultimately we require a robust means to isolate the different contributors to the iron cycle within a
306 holistic physical framework (Box 1, Figure 4a), as exists for major nutrients. This would allow the
307 global significance of ocean physics, regeneration and scavenging to iron distributions to be jointly
308 elucidated⁶⁹. With this approach, the first order levels of coupling and decoupling between iron and
309 major nutrients like phosphate may be quantified for use in parameterising the foundations of
310 global models. Furthermore, considering iron observations within their physical context, e.g. water
311 masses, density or potential vorticity, will facilitate the quantification of the rates of key processes.
312 Exploiting the coherent iron-hydrography datasets from GEOTRACES and targeted process
313 studies is needed to achieve this goal.

314 315 **3.2 Which iron pools underpin variations in iron cycling?**

316
317 While the new synthesis (Fig 2) expands our understanding of how iron links to wider
318 biogeochemical cycling, the underlying processes themselves are ultimately governed by the
319 particular functional forms of iron that define its 'reactivity'. It is important to consider reactivity in
320 different ways depending on particular process. Biological reactivity (or bioavailability) affects the
321 ability of the biota to acquire iron or how bacteria remineralise iron from organic material, while
322 chemical reactivity will modulate the dissolution of lithogenic iron and the propensity of different
323 forms of iron to be transferred to particulate pools via scavenging or colloidal aggregation. A key
324 contrast between iron and the major nutrients is that while specific chemical forms of nitrogen (e.g.
325 nitrate) or phosphorus (e.g. phosphate) are measured, iron measurements rely on operational
326 definitions. The prime focus of ocean iron observations remains on separating 'dissolved' and
327 particulate iron, i.e. all forms of iron that pass through (or are retained by) a defined filter (normally
328 0.2 μm). However, somewhere between half and three quarters of dissolved iron does not pass a
329 smaller 0.02 μm filter, which has led to a further distinction between 'soluble' and 'colloidal'
330 dissolved iron⁹⁴.

331
332 Until relatively recently, most of the focus on the iron present in these different size fractions has
333 been from a geochemical or chemical perspective on inorganic species - emphasising the degree
334 of complexation between iron and ligands in soluble and colloidal pools⁹⁴ or the solubility and
335 mineralogy of colloidal and particulate iron⁹⁵. However, due to the scarcity and bio-essential nature
336 of iron, much of the iron reservoir must be associated with the biota and their biochemical
337 components. For instance, phytoplankton and bacteria are a notable fraction of the small
338 particulate iron pool⁹⁶, while the virus-associated iron may be a non-negligible component of
339 colloidal iron⁹⁷. Additionally, intracellular iron, that is largely associated with metalloenzymes and
340 storage proteins⁹⁸ will be released to the dissolved phase following microbial grazing and viral lysis
341 of biogenic particles. Notable examples of biomolecules that may contribute to the dissolved or

342 colloidal iron pool when released from cells include numerous metalloenzymes and their iron-
343 binding constituents (e.g. hemes and iron-sulphur clusters)⁹⁹, as well as ferritin and bacteroferritin
344 (iron storage proteins)⁹⁸. While the magnitude of their contribution to measured iron levels and their
345 lifetime in the dissolved phase remain unknown, these biogenic iron species will contribute to the
346 biological and chemical reactivity of iron in different environments. On-going work with new ultra
347 high mass resolution mass spectrometry and 'omics based studies are delving deeper into the
348 'black box' of what makes up different iron pools, which will be crucial in better understanding the
349 biological and/or chemical reactivity of iron. A key challenge in this regard is the transient nature of
350 these different components of the ocean iron pool, which is affected by the specific attributes of
351 distinct environments and will ultimately regulate the linkages between iron and other
352 biogeochemical cycles (Fig 4b).

353

354 **3.3. Transcending the scale window: New frontiers for the ocean iron cycle**

355

356 Will we see the same step change in our understanding of the ocean iron cycle over the next
357 decade? The importance of iron in regulating ocean productivity and biogeochemical cycling is well
358 established and as we have discussed, important aspects unique to its oceanic cycling, relative to
359 major nutrients, have been identified (Figs 2 and 3). Thus to be able to project the impacts of
360 ocean change with confidence, iron needs to be fully integrated into a theoretical framework where
361 the main drivers of its distribution and cycling are identified, as for major nutrients. This would
362 enable progress to be made in the representation of iron cycling in the ocean models we rely on to
363 test hypotheses and appraise the consequences of on-going climate change. Enormous progress
364 has been made in our ability to observe ocean iron distributions thanks to GEOTRACES, but better
365 understanding of the roles played by different biological, chemical and physical processes remains
366 elusive. In part this is due to our fragmentary picture of ocean iron cycle variability and the linkages
367 to global biogeochemical cycles.

368

369 When iron measurements are conducted at similar scales to other biogeochemical tracers during
370 targeted experiments, budgets and fluxes can be quantified, which yield insight into the linkages
371 that ultimately regulate the functioning of the ocean's biogeochemical cycles. For example, the
372 FeCycle experiment followed iron dynamics in a labelled patch of the subantarctic Southern
373 Ocean, documenting the parallel roles of ocean physics, biology and chemistry in governing links
374 between iron and broader aspects of biogeochemical cycling, including dust iron supply⁴⁴. Two
375 multi-disciplinary experiments focussing on the naturally fertilised Kerguelen plateau region in
376 different seasons were able to develop regional iron budgets⁷⁵ and make wider links to physical
377 and biological processes, including downward biogenic carbon export and air-sea CO₂ exchange.
378 We recommend future work that expands such efforts to the ocean basin scale, coupling ocean
379 sections with insights into the associated physical, chemical, biochemical and ecological
380 processes. This may be achieved in its simplest sense by expanding the biological, biochemical
381 and physical measurements conducted on GEOTRACES sections, as for the GA03 north Atlantic
382 section^{72,92}. More ambitiously, key regions along sections (e.g. downstream of iron sources or
383 across gradients of iron stress) may be targeted and controlled volume experiments performed to
384 elucidate the governing processes. Finally, expanding the temporal scale of iron sampling requires
385 advances in analytical chemistry, which may ultimately yield the autonomous sensors or remote
386 samplers for iron needed to transform our ability to observe variability (e.g. at time-series stations).
387 For instance, this could illuminate how natural climate variations (e.g. El Nino in the Pacific) or
388 seasonal transitions (e.g. at high latitudes or in coastal upwellings) shape biogeochemical cycles
389 via modifications to iron dynamics.

390

391 **Figure Legends**

392

393 **Figure 1.** A schematic representation of the first view of the processes governing the ocean iron
394 cycle. The major external source is dust, with the iron supplied from continental margins and
395 hydrothermal activity on mid ocean ridges thought to be lost from the dissolved pool close to the
396 source. Release of iron from dust or supply from upwelling stimulates biological activity, nitrogen
397 fixation and particulate organic matter fluxes in a constant relationship to major nutrients. In the
398 ocean interior, iron regeneration and scavenging is controlled by fixed concentrations of iron
399 binding organic ligands.

400

401 **Figure 2.** A revised representation of the major processes in the ocean iron cycle. A broad
402 meridional contrast is emphasised between the iron-limited Southern Ocean and the major nutrient
403 limited low latitude regimes. Dust remains dominant in the low latitudes, but continental margin
404 and upwelled hydrothermal sources are more important in the Southern Ocean. Flexible iron
405 uptake and biological cycling, along with the production of excess iron binding ligands dominate
406 the Southern Ocean, whereas nitrogen fixation occurs in the low latitudes (although this process
407 can also be restricted by lack of iron outside of the north Atlantic subtropical gyre). The particulate
408 organic iron flux is decoupled from that of phosphorus at high latitudes and the flux of lithogenic
409 material is important at low latitudes influenced by dust. Subduction of excess organic iron binding
410 ligands from the Southern Ocean has a remote influence on the interior ocean at low latitudes.

411

412 **Figure 3.** Dissolved phosphate (upper panel) and dissolved iron (lower panel) observations
413 collected along the GA02 GEOTRACES meridional section in the west Atlantic⁸⁵ as a function of
414 latitude, with contours of constant potential vorticity overlain.

415

416 **Figure 4.** a) A schematic representation of how iron cycle processes can be placed within a
417 holistic physical framework. Subduction of a water mass between density layers (σ_1 and σ_2) and
418 subsequent spreading along lines of constant potential vorticity transports iron signals. This remote
419 impact will then affect the interpretation of observed local phenomena. The terminology of the iron
420 and ligand pools is described in Box 1. b) An illustration of the different components of particulate
421 and dissolved iron (including the soluble and colloidal components Emphasis is on a fluid
422 continuum of soluble, colloidal and particulate iron, as well as the role of inorganic (bottom
423 half: nano particles and lithogenic species) and organic components (top half: encompassing
424 biogenic and biomolecules that bind iron strongly, as well as weaker diffuse iron-binding ligands
425 such as hemes, saccharides or fulvic acids).

426

Box 1: Using theory to identify first order governing processes

A suite of interleaving processes controls the distributions of nutrients in the ocean. Biological uptake and chemical removal constitute sinks, whereas external inputs and regeneration are sources. Physical transport also transfers nutrients between surface and deep waters and throughout the ocean interior. Thus, interior ocean phosphate (P_{TOT}) is the sum of preformed (physically transported into the ocean interior, P_{PRE}) and regenerated (i.e. from sinking organic matter, P_{REG}) pools:

$$P_{TOT} = P_{PRE} + P_{REG} \quad (1)$$

P_{REG} is quantified using apparent oxygen utilisation (AOU) and the phosphate:oxygen ratio ($R_{P:O_2}$):

$$P_{REG} = R_{P:O_2} AOU \quad (2)$$

Equations 1 and 2 then quantify the varying influences of ocean circulation and biological activity on phosphorus cycling^{100,101}. As the biological pump shifts phosphorus from the preformed to the regenerated pool, P_{REG}/P_{TOT} (known as P^*) quantifies the efficiency of the biological pump¹⁰⁰. Observations indicate that the biological pump operates at around one-third efficiency, with a linear relationship between P^* and atmospheric CO_2 levels¹⁰⁰. This theory underpins the 'iron hypothesis'¹⁹, whereby additional iron enhances the biological pump efficiency by shifting extra phosphate from the preformed to the regenerated pool and lowering CO_2 .

While a similar theory for iron (Fe_{TOT}) would include preformed (Fe_{PRE}) and regenerated (Fe_{REG}) components, it must also consider subsurface sediment (Fe_{SED}) and hydrothermal (Fe_{HYD}) input, alongside iron scavenging loss (Fe_{SCAV}). The dust iron deposited within the mixed layer affects Fe_{PRE} , but the smaller amount of dust that dissolves in the ocean interior (Fe_{DUST}) must be included:

$$Fe_{TOT} = Fe_{PRE} + Fe_{REG} + Fe_{SED} + Fe_{HYD} + Fe_{DUST} - Fe_{SCAV} \quad (3)$$

Variability in the iron content of sinking organic matter⁷¹ causes a variable $R_{Fe:O_2}$ that must be combined with AOU to derive Fe_{REG} . Using Equation 3 within a model finds that Fe_{PRE} interacts with interior sources to shape the magnitude of surface iron supply⁶⁹ (Fig 2). Importantly, the regeneration and scavenging balance (i.e. $Fe_{REG} - Fe_{SCAV}$) is decoupled from the gross rates of regeneration inferred from AOU because upstream subduction of excess ligands places an upper limit on how regeneration impacts total iron⁶⁹. This explains why the slope of the dissolved iron to AOU relationship differs from phytoplankton iron contents⁷². While AOU itself may not be the ideal tracer of remineralisation rates, it offers a tractable means for its basin scale quantification.

If Equation 3 were linked to observations, the first order drivers of the ocean iron cycle could be identified. This can be achieved if estimates of phytoplankton iron content^{72,77} are allied to ocean tracers (Sec 3.1). For instance, linking subduction timescales determined from transient tracers to density-based or potential vorticity flow pathways can track preformed iron and its modification. Source-specific tracers, such as helium or radium may isolate hydrothermal and sediment pools. Interior dissolution of dust may be traced via lithogenic tracers such as aluminium and titanium. Finally, other particle reactive elements that are not biologically active (e.g. thorium) can constrain scavenging.

Ultimately, the role of the each term in Equation 3 is affected by organic iron-binding ligands⁶⁹ that are usually in excess of iron⁶³. A parallel approach for the total ligand concentration (L_{TOT}) should account for preformed surface produced ligands (L_{PRE}), interior ligand production from both organic matter degradation (L_{REG}) or specific sources (L_{SOURCE}), and ligand loss (L_{LOSS}) from bacterial decay and coagulation:

$$L_{TOT} = L_{PRE} + L_{REG} + L_{SOURCE} - L_{LOSS} \quad (4)$$

484 Equation 4 may be quantified by combining experimental studies and tracers, but an important and
485 confounding issue is the diversity of ligands present (i.e. a blend of iron binding molecules typically
486 represented as distinct 'classes' based on measured binding constants), since each may have a
487 unique provenance and impact(s) on the iron cycle⁶²⁻⁶⁴.
488

489 **References**

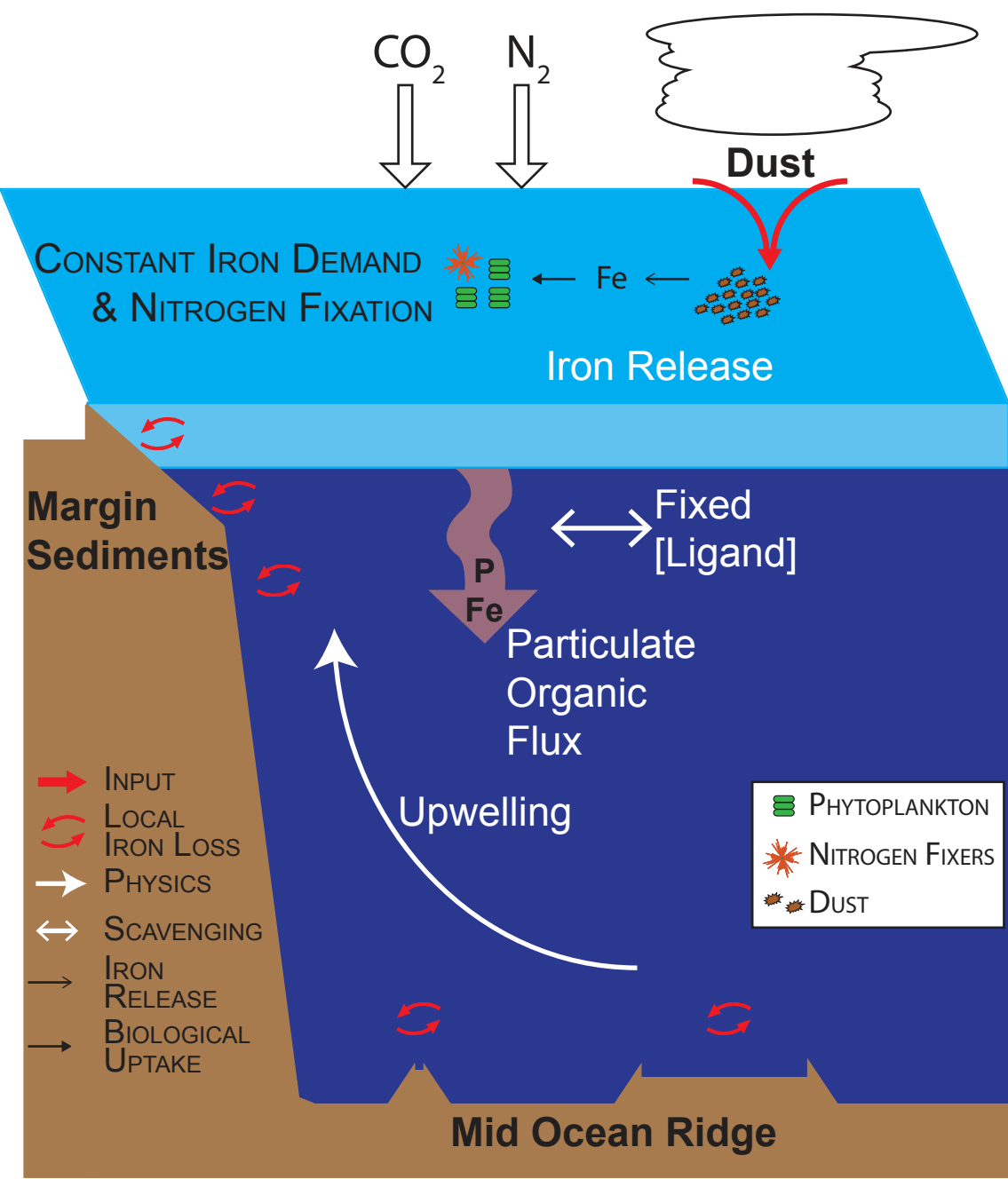
- 490
- 491 1 Falkowski, P. & Raven, J. A. *Aquatic Photosynthesis*. 488 (Princeton University Press,
- 492 2007).
- 493 2 Ruud, J. T. Nitrates and phosphates in the Southern Seas. *Journal du Conseil* **5**, 347-360
- 494 (1930).
- 495 3 Gran, H. H. On the conditions for the production of plankton in the sea. *Conseil Perm.*
- 496 *Internat. pour l'Explor. de la Mer. Rapp. et Proces-Verb.* **75**, 37-46 (1931).
- 497 4 Hart, T. On the phytoplankton of the south-west Atlantic and the Bellingshausen Sea, 1929-
- 498 31. *Discovery Reports* **VIII**, 1-268 (1934).
- 499 5 Harvey, H. On the rate of diatom growth. *Journ. Mar. Biol. Assoc* **19**, 253-276 (1933).
- 500 6 Anderson, M. A. & Morel, F. M. M. The influence of aqueous iron chemistry on the uptake
- 501 of iron by the coastal diatom *Thalassiosira weissflogii* 1. *Limnology and Oceanography* **27**,
- 502 789-813, doi:10.4319/lo.1982.27.5.0789 (1982).
- 503 7 Brand, L. E., Sunda, W. G. & Guillard, R. R. L. Limitation of marine phytoplankton
- 504 reproductive rates by zinc, manganese and iron. *Limnology and Oceanography* **28**, 1182-
- 505 1198, doi:10.4319/lo.1983.28.6.1182 (1983).
- 506 8 Cooper, L. H. N. Iron in the Sea and in Marine Plankton. *Proceedings of the Royal Society*
- 507 *B: Biological Sciences* **118**, 419-438, doi:10.1098/rspb.1935.0064 (1935).
- 508 9 Goldberg, E. D. Marine Geochemistry 1. Chemical Scavengers of the Sea. *The Journal of*
- 509 *Geology* **62**, 249-265, doi:10.1086/626161 (1954).
- 510 10 Williams, R. J. P. The Bakerian Lecture, 1981 - Natural-Selection of the Chemical-
- 511 Elements. *Proc R Soc Ser B-Bio* **213**, 361-397, doi:10.1098/rspb.1981.0071 (1981).
- 512 11 Raven, J. A. The iron and molybdenum use efficiencies of plant growth with different
- 513 energy, carbon and nitrogen sources. *New Phytologist* **109**, 279-287, doi:10.1111/j.1469-
- 514 8137.1988.tb04196.x (1988).
- 515 12 Moore, J. K., Doney, S. C., Glover, D. M. & Fung, I. Y. Iron cycling and nutrient-limitation
- 516 patterns in surface waters of the World Ocean. *Deep-Sea Res Pt II* **49**, 463-507,
- 517 doi:10.1016/S0967-0645(01)00109-6 (2002).
- 518 13 Bruland, K. W., Franks, R. P., Knauer, G. A. & Martin, J. H. Sampling and analytical
- 519 methods for the determination of copper, cadmium, zinc, and nickel at the nanogram per
- 520 liter level in sea water. *Analytica chimica acta* **105**, 233-245, doi:10.1016/s0003-
- 521 2670(01)83754-5 (1979).
- 522 14 Settle, D. & Patterson, C. Lead in albacore: guide to lead pollution in Americans. *Science*
- 523 **207**, 1167-1176, doi:10.1126/science.6986654 (1980).
- 524 15 Gordon, R. M., Martin, J. H. & Knauer, G. A. Iron in Northeast Pacific Waters. *Nature* **299**,
- 525 611-612, doi:10.1038/299611a0 (1982).
- 526 16 Landing, W. M. & Bruland, K. W. The contrasting biogeochemistry of iron and manganese
- 527 in the Pacific Ocean. *Geochimica et Cosmochimica Acta* **51**, 29-43, doi:10.1016/0016-
- 528 7037(87)90004-4 (1987).
- 529 17 Martin, J. H., Gordon, R. M. & Fitzwater, S. E. Iron in Antarctic Waters. *Nature* **345**, 156-
- 530 158, doi:10.1038/345156a0 (1990).
- 531 18 Martin, J. H., Fitzwater, S. E. & Gordon, R. M. Iron deficiency limits phytoplankton growth in
- 532 Antarctic waters. *Global Biogeochemical Cycles* **4**, 5-12, doi:10.1029/GB004i001p00005
- 533 (1990).
- 534 19 Martin, J. H. Glacial-Interglacial Co₂ Change: The Iron Hypothesis. *Paleoceanography* **5**, 1-
- 535 13, doi:10.1029/Pa005i001p00001 (1990).
- 536 20 Joos, F., Sarmiento, J. L. & Siegenthaler, U. Estimates of the effect of Southern Ocean iron
- 537 fertilization on atmospheric CO₂ concentrations. *Nature* **349**, 772-775,
- 538 doi:10.1038/349772a0 (1991).
- 539 21 Cullen, J. J. Hypotheses to explain high-nutrient conditions in the open sea. *Limnology and*
- 540 *Oceanography* **36**, 1578-1599, doi:10.4319/lo.1991.36.8.1578 (1991).
- 541 22 Martin, J. H. *et al.* Testing the Iron Hypothesis in Ecosystems of the Equatorial Pacific-
- 542 Ocean. *Nature* **371**, 123-129, doi:10.1038/371123a0 (1994).
- 543 23 Coale, K. H. *et al.* A massive phytoplankton bloom induced by an ecosystem-scale iron
- 544 fertilization experiment in the equatorial Pacific Ocean. *Nature* **383**, 495-501,
- 545 doi:10.1038/383495a0 (1996).

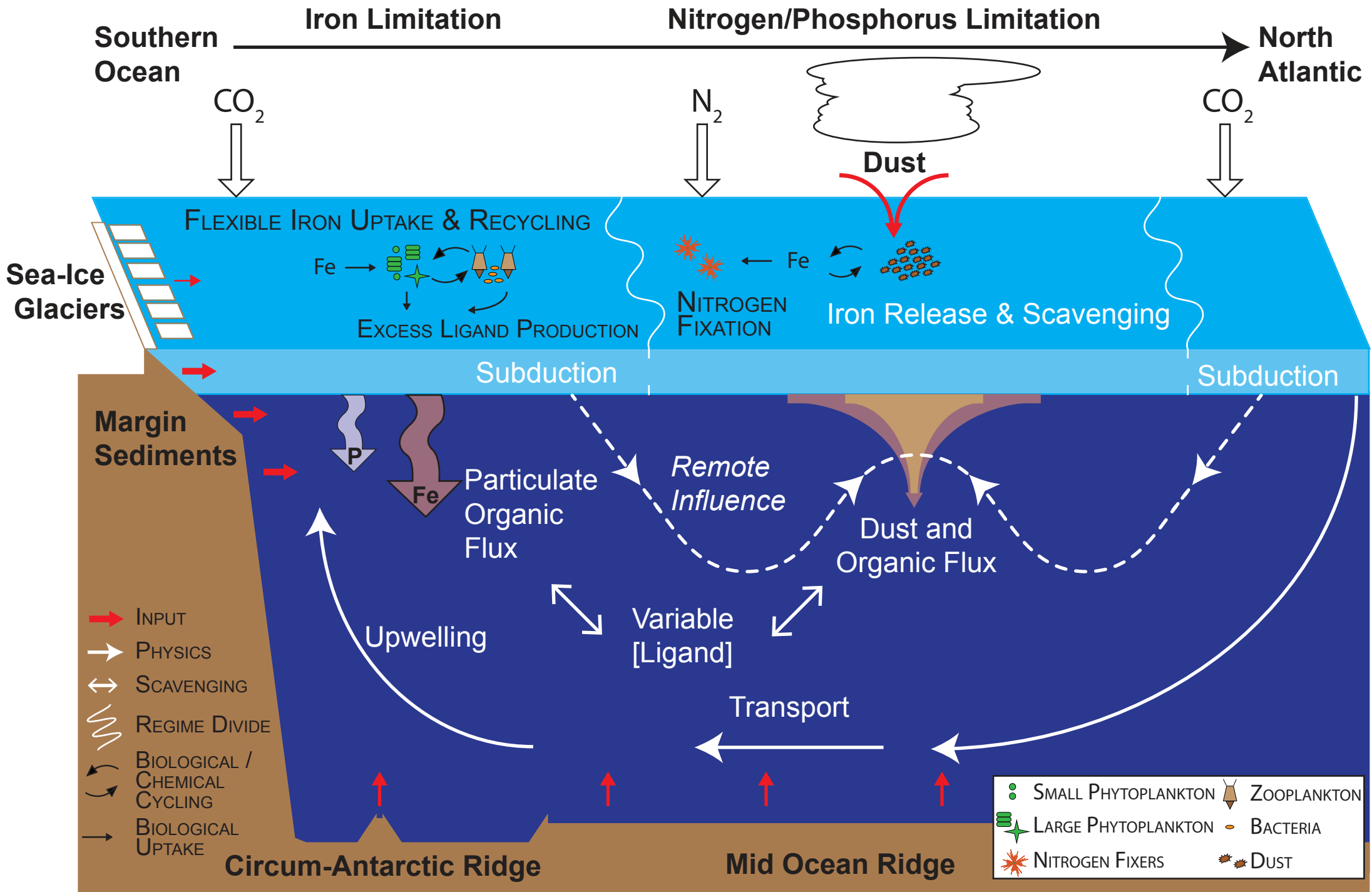
- 546 24 Boyd, P. W. *et al.* A mesoscale phytoplankton bloom in the polar Southern Ocean
547 stimulated by iron fertilization. *Nature* **407**, 695-702, doi:10.1038/35037500 (2000).
- 548 25 Boyd, P. W. *et al.* Mesoscale iron enrichment experiments 1993-2005: Synthesis and future
549 directions. *Science* **315**, 612-617, doi:10.1126/Science.1131669 (2007).
- 550 26 de Baar, H. J. W. *et al.* Synthesis of iron fertilization experiments: From the Iron Age in the
551 Age of Enlightenment. *Journal of Geophysical Research* **110**, doi:10.1029/2004jc002601
552 (2005).
- 553 27 Moore, C. M. *et al.* Iron limits primary productivity during spring bloom development in the
554 central North Atlantic. *Global Change Biology* **12**, 626-634, doi:10.1111/j.1365-
555 2486.2006.01122.x (2006).
- 556 28 Hutchins, D. A., DiTullio, G. R., Zhang, Y. & Bruland, K. W. An iron limitation mosaic in the
557 California upwelling regime. *Limnology and Oceanography* **43**, 1037-1054,
558 doi:10.4319/lo.1998.43.6.1037 (1998).
- 559 29 Hutchins, D. A. *et al.* Phytoplankton iron limitation in the Humboldt Current and Peru
560 Upwelling. *Limnology and Oceanography* **47**, 997-1011, doi:10.4319/lo.2002.47.4.0997
561 (2002).
- 562 30 Johnson, K. S., Gordon, R. M. & Coale, K. H. What controls dissolved iron concentrations
563 in the world ocean? *Marine Chemistry* **57**, 137-161, doi:10.1016/s0304-4203(97)00043-1
564 (1997).
- 565 31 Gledhill, M. & van den Berg, C. M. G. Determination of complexation of iron(III) with natural
566 organic complexing ligands in seawater using cathodic stripping voltammetry. *Marine*
567 *Chemistry* **47**, 41-54, doi:10.1016/0304-4203(94)90012-4 (1994).
- 568 32 Rue, E. L. & Bruland, K. W. Complexation of iron(III) by natural organic ligands in the
569 Central North Pacific as determined by a new competitive ligand equilibration/adsorptive
570 cathodic stripping voltammetric method. *Marine Chemistry* **50**, 117-138, doi:10.1016/0304-
571 4203(95)00031-1 (1995).
- 572 33 Sunda, W. G. & Huntsman, S. A. Interrelated influence of iron, light and cell size on marine
573 phytoplankton growth. *Nature* **390**, 389-392, doi:10.1038/37093 (1997).
- 574 34 Archer, D. E. & Johnson, K. A model of the iron cycle in the ocean. *Global Biogeochemical*
575 *Cycles* **14**, 269-279, doi:10.1029/1999gb900053 (2000).
- 576 35 Parekh, P., Follows, M. J. & Boyle, E. A. Decoupling of iron and phosphate in the global
577 ocean. *Global Biogeochemical Cycles* **19**, doi:10.1029/2004gb002280 (2005).
- 578 36 Jickells, T. D. *et al.* Global iron connections between desert dust, ocean biogeochemistry,
579 and climate. *Science* **308**, 67-71, doi:10.1126/Science.1105959 (2005).
- 580 37 de Baar, H. J. & de Jong, J. T. in *The biogeochemistry of iron in seawater* Vol. 7 (eds D. R.
581 Turner & K. A. Hunter) 123-254 (2001).
- 582 38 Tagliabue, A. *et al.* How well do global ocean biogeochemistry models simulate dissolved
583 iron distributions? *Global Biogeochemical Cycles*, doi:10.1002/2015gb005289 (2016).
- 584 39 Hain, M. P., Sigman, D. M. & Haug, G. H. Carbon dioxide effects of Antarctic stratification,
585 North Atlantic Intermediate Water formation, and subantarctic nutrient drawdown during the
586 last ice age: Diagnosis and synthesis in a geochemical box model. *Global Biogeochemical*
587 *Cycles* **24**, doi:10.1029/2010gb003790 (2010).
- 588 40 Watson, A. J., Bakker, D. C. E., Ridgwell, A. J., Boyd, P. W. & Law, C. S. Effect of iron
589 supply on Southern Ocean CO₂ uptake and implications for glacial atmospheric CO₂.
590 *Nature* **407**, 730-733, doi:10.1038/35037561 (2000).
- 591 41 Mawji, E. *et al.* The GEOTRACES Intermediate Data Product 2014. *Marine Chemistry* **177**,
592 1-8, doi:10.1016/j.marchem.2015.04.005 (2015).
- 593 42 Anderson, R. & Henderson, G. GEOTRACES—A Global Study of the Marine
594 Biogeochemical Cycles of Trace Elements and Their Isotopes. *Oceanography* **18**, 76-79,
595 doi:10.5670/oceanog.2005.31 (2005).
- 596 43 Johnson, K. S. *et al.* Developing Standards for Dissolved Iron in Seawater. *Eos*,
597 *Transactions American Geophysical Union* **88**, 131, doi:10.1029/2007eo110003 (2007).
- 598 44 Boyd, P. W. *et al.* FeCycle: Attempting an iron biogeochemical budget from a mesoscale
599 SF₆ tracer experiment in unperturbed low iron waters. *Global Biogeochemical Cycles* **19**,
600 doi:10.1029/2005gb002494 (2005).
- 601 45 Blain, S. *et al.* Effect of natural iron fertilization on carbon sequestration in the Southern
602 Ocean. *Nature* **446**, 1070-U1071, doi:10.1038/Nature05700 (2007).

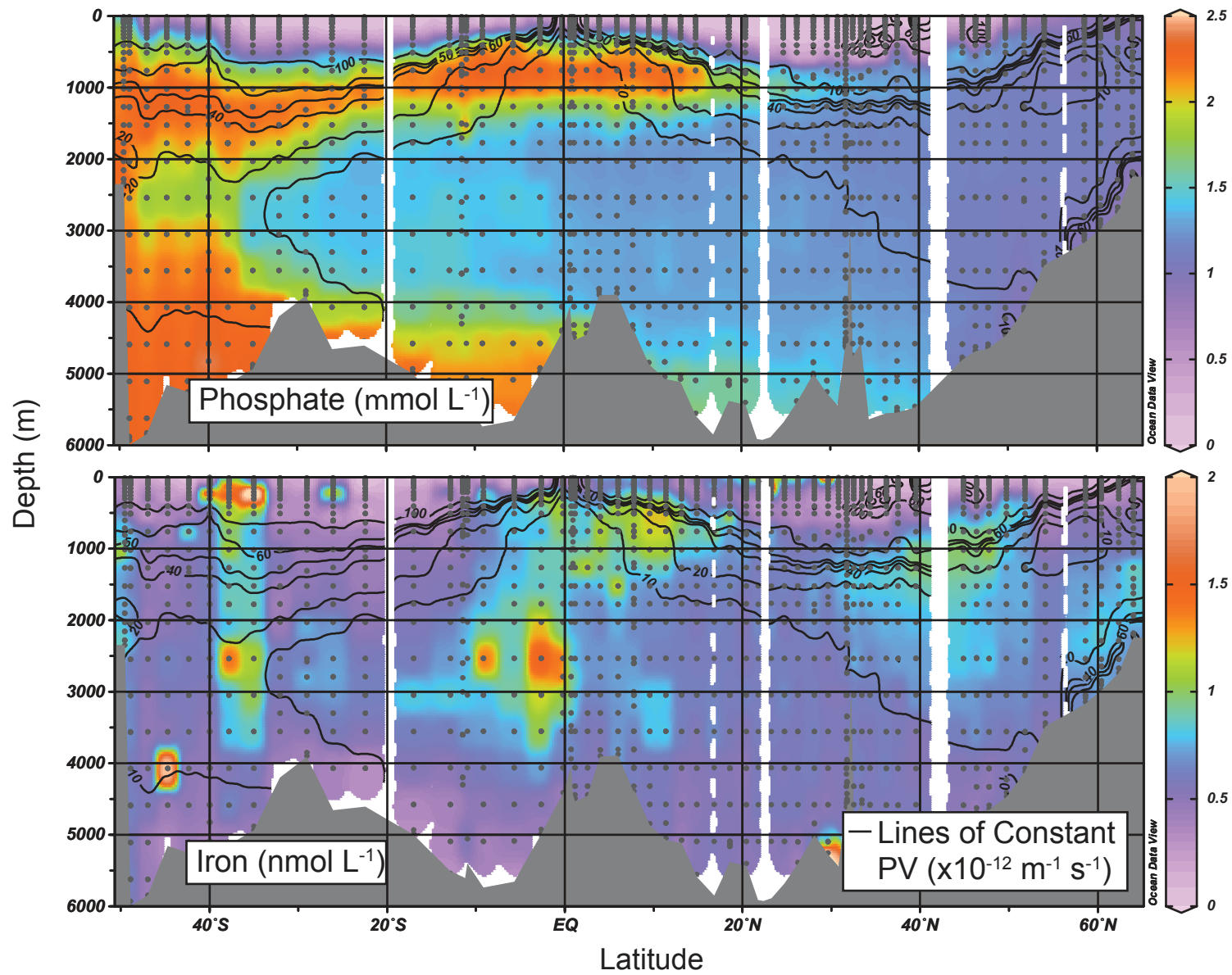
- 603 46 Pollard, R. T. *et al.* Southern Ocean deep-water carbon export enhanced by natural iron
604 fertilization. *Nature* **457**, 577-580, doi:10.1038/nature07716 (2009).
- 605 47 Elrod, V. A., Berelson, W. M., Coale, K. H. & Johnson, K. S. The flux of iron from
606 continental shelf sediments: A missing source for global budgets. *Geophysical Research*
607 *Letters* **31**, doi:10.1029/2004gl020216 (2004).
- 608 48 Lam, P. J. & Bishop, J. K. B. The continental margin is a key source of iron to the HNLC
609 North Pacific Ocean. *Geophysical Research Letters* **35**, doi:10.1029/2008gl033294 (2008).
- 610 49 Tagliabue, A., Aumont, O. & Bopp, L. The impact of different external sources of iron on the
611 global carbon cycle. *Geophysical Research Letters* **41**, 920-926,
612 doi:10.1002/2013gl059059 (2014).
- 613 50 Saito, M. A. *et al.* Slow-spreading submarine ridges in the South Atlantic as a significant
614 oceanic iron source. *Nature Geoscience* **6**, 775-779, doi:10.1038/Ngeo1893 (2013).
- 615 51 Resing, J. A. *et al.* Basin-scale transport of hydrothermal dissolved metals across the South
616 Pacific Ocean. *Nature* **523**, 200-203, doi:10.1038/nature14577 (2015).
- 617 52 Klunder, M. B., Laan, P., Middag, R., De Baar, H. J. W. & van Ooijen, J. C. Dissolved iron
618 in the Southern Ocean (Atlantic sector). *Deep Sea Research Part II: Topical Studies in*
619 *Oceanography* **58**, 2678-2694, doi:10.1016/j.dsr2.2010.10.042 (2011).
- 620 53 Klunder, M. B. *et al.* Dissolved iron in the Arctic shelf seas and surface waters of the central
621 Arctic Ocean: Impact of Arctic river water and ice-melt. *J Geophys Res-Oceans* **117**,
622 doi:10.1029/2011jc007133 (2012).
- 623 54 Tagliabue, A. *et al.* Hydrothermal contribution to the oceanic dissolved iron inventory.
624 *Nature Geoscience* **3**, 252-256, doi:10.1038/ngeo818 (2010).
- 625 55 Conway, T. M. & John, S. G. Quantification of dissolved iron sources to the North Atlantic
626 Ocean. *Nature* **511**, 212-215, doi:10.1038/nature13482 (2014).
- 627 56 Moore, C. M. *et al.* Processes and patterns of oceanic nutrient limitation. *Nature*
628 *Geoscience*, doi:10.1038/ngeo1765 (2013).
- 629 57 Falkowski, P. G. Evolution of the nitrogen cycle and its influence on the biological
630 sequestration of CO₂ in the ocean. *Nature* **387**, 272-275, doi:10.1038/387272a0 (1997).
- 631 58 Moore, C. M. *et al.* Large-scale distribution of Atlantic nitrogen fixation controlled by iron
632 availability. *Nature Geoscience* **2**, 867-871, doi:10.1038/ngeo667 (2009).
- 633 59 Schlosser, C. *et al.* Seasonal ITCZ migration dynamically controls the location of the
634 (sub)tropical Atlantic biogeochemical divide. *Proceedings of the National Academy of*
635 *Sciences of the United States of America* **111**, 1438-1442, doi:10.1073/pnas.1318670111
636 (2014).
- 637 60 Dutkiewicz, S., Ward, B. A., Monteiro, F. & Follows, M. J. Interconnection of nitrogen fixers
638 and iron in the Pacific Ocean: Theory and numerical simulations. *Global Biogeochemical*
639 *Cycles* **26**, doi:10.1029/2011gb004039 (2012).
- 640 61 Weber, T. & Deutsch, C. Local versus basin-scale limitation of marine nitrogen fixation.
641 *Proceedings of the National Academy of Sciences of the United States of America* **111**,
642 8741-8746, doi:10.1073/pnas.1317193111 (2014).
- 643 62 Gledhill, M. & Buck, K. N. The organic complexation of iron in the marine environment: a
644 review. *Frontiers in microbiology* **3**, 69, doi:10.3389/fmicb.2012.00069 (2012).
- 645 63 Boyd, P. W. & Tagliabue, A. Using the L* concept to explore controls on the relationship
646 between paired ligand and dissolved iron concentrations in the ocean. *Marine Chemistry*
647 **173**, 52-66, doi:10.1016/j.marchem.2014.12.003 (2015).
- 648 64 Buck, K. N., Sohst, B. & Sedwick, P. N. The organic complexation of dissolved iron along
649 the U.S. GEOTRACES (GA03) North Atlantic Section. *Deep Sea Research Part II: Topical*
650 *Studies in Oceanography* **116**, 152-165, doi:10.1016/j.dsr2.2014.11.016 (2015).
- 651 65 Gerringa, L. J. A., Rijkenberg, M. J. A., Schoemann, V., Laan, P. & de Baar, H. J. W.
652 Organic complexation of iron in the West Atlantic Ocean. *Marine Chemistry* **177**, 434-446,
653 doi:10.1016/j.marchem.2015.04.007 (2015).
- 654 66 Wozniak, A. S., Shelley, R. U., McElhenie, S. D., Landing, W. M. & Hatcher, P. G. Aerosol
655 water soluble organic matter characteristics over the North Atlantic Ocean: Implications for
656 iron-binding ligands and iron solubility. *Marine Chemistry* **173**, 162-172,
657 doi:10.1016/j.marchem.2014.11.002 (2015).
- 658 67 Cheize, M. *et al.* Iron organic speciation determination in rainwater using cathodic stripping
659 voltammetry. *Analytica chimica acta* **736**, 45-54, doi:10.1016/j.aca.2012.05.011 (2012).

- 660 68 Mawji, E. *et al.* Production of siderophore type chelates in Atlantic Ocean waters enriched
661 with different carbon and nitrogen sources. *Marine Chemistry* **124**, 90-99,
662 doi:10.1016/j.marchem.2010.12.005 (2011).
- 663 69 Tagliabue, A., Williams, R. G., Rogan, N., Achterberg, E. P. & Boyd, P. W. A ventilation-
664 based framework to explain the regeneration-scavenging balance of iron in the ocean.
665 *Geophysical Research Letters* **41**, 7227-7236, doi:10.1002/2014gl061066 (2014).
- 666 70 Völker, C. & Tagliabue, A. Modeling organic iron-binding ligands in a three-dimensional
667 biogeochemical ocean model. *Marine Chemistry* **173**, 67-77,
668 doi:10.1016/j.marchem.2014.11.008 (2015).
- 669 71 Twining, B. S. & Baines, S. B. The trace metal composition of marine phytoplankton.
670 *Annual review of marine science* **5**, 191-215, doi:10.1146/annurev-marine-121211-172322
671 (2013).
- 672 72 Twining, B. S., Rauschenberg, S., Morton, P. L. & Vogt, S. Metal contents of phytoplankton
673 and labile particulate material in the North Atlantic Ocean. *Progress in Oceanography* **137**,
674 261-283, doi:10.1016/j.pocean.2015.07.001 (2015).
- 675 73 Martiny, A. C. *et al.* Strong latitudinal patterns in the elemental ratios of marine plankton
676 and organic matter. *Nature Geoscience* **6**, 279-283, doi:10.1038/ngeo1757 (2013).
- 677 74 Boyd, P. W. *et al.* Why are biotic iron pools uniform across high- and low-iron pelagic
678 ecosystems? *Global Biogeochemical Cycles* **29**, 1028-1043, doi:10.1002/2014gb005014
679 (2015).
- 680 75 Bowie, A. R. *et al.* Iron budgets for three distinct biogeochemical sites around the
681 Kerguelen Archipelago (Southern Ocean) during the natural fertilisation study, KEOPS-2.
682 *Biogeosciences* **12**, 4421-4445, doi:10.5194/bg-12-4421-2015 (2015).
- 683 76 Ratnarajah, L., Bowie, A. R., Lannuzel, D., Meiners, K. M. & Nicol, S. The biogeochemical
684 role of baleen whales and krill in Southern Ocean nutrient cycling. *Plos One* **9**, e114067,
685 doi:10.1371/journal.pone.0114067 (2014).
- 686 77 Twining, B. S. *et al.* Differential remineralization of major and trace elements in sinking
687 diatoms. *Limnol. Oceanogr* **59**, 689-704, doi:10.4319/lo.2014.59.3.0689 (2014).
- 688 78 Tagliabue, A. *et al.* Surface-water iron supplies in the Southern Ocean sustained by deep
689 winter mixing. *Nature Geoscience* **7**, 314-320, doi:10.1038/ngeo2101 (2014).
- 690 79 Hudson, R. J. M. & Morel, F. M. M. Iron transport in marine phytoplankton: Kinetics of
691 cellular and medium coordination reactions. *Limnology and Oceanography* **35**, 1002-1020,
692 doi:10.4319/lo.1990.35.5.1002 (1990).
- 693 80 Morel, F. M. M., Kustka, A. B. & Shaked, Y. The role of unchelated Fe in the iron nutrition of
694 phytoplankton. *Limnology and Oceanography* **53**, 400-404, doi:10.4319/lo.2008.53.1.0400
695 (2008).
- 696 81 Strzepek, R. F., Maldonado, M. T., Hunter, K. A., Frew, R. D. & Boyd, P. W. Adaptive
697 strategies by Southern Ocean phytoplankton to lessen iron limitation: Uptake of organically
698 complexed iron and reduced cellular iron requirements. *Limnology and Oceanography* **56**,
699 1983-2002, doi:10.4319/lo.2011.56.6.1983 (2011).
- 700 82 Maldonado, M. T. & Price, N. M. Utilization of iron bound to strong organic ligands by
701 plankton communities in the subarctic Pacific Ocean. *Deep Sea Research Part II: Topical
702 Studies in Oceanography* **46**, 2447-2473, doi:10.1016/s0967-0645(99)00071-5 (1999).
- 703 83 Rubin, M., Berman-Frank, I. & Shaked, Y. Dust- and mineral-iron utilization by the marine
704 dinitrogen-fixer *Trichodesmium*. *Nature Geoscience* **4**, 529-534, doi:10.1038/ngeo1181
705 (2011).
- 706 84 Saito, M. A. *et al.* Multiple nutrient stresses at intersecting Pacific Ocean biomes detected
707 by protein biomarkers. *Science* **345**, 1173-1177, doi:10.1126/science.1256450 (2014).
- 708 85 Rijkenberg, M. J. *et al.* The distribution of dissolved iron in the West Atlantic Ocean. *Plos
709 One* **9**, e101323, doi:10.1371/journal.pone.0101323 (2014).
- 710 86 Wagener, T., Guieu, C. & Leblond, N. Effects of dust deposition on iron cycle in the surface
711 Mediterranean Sea: results from a mesocosm seeding experiment. *Biogeosciences* **7**,
712 3769-3781, doi:Doi 10.5194/Bg-7-3769-2010 (2010).
- 713 87 Sohm, J. A. *et al.* Nitrogen fixation in the South Atlantic Gyre and the Benguela Upwelling
714 System. *Geophysical Research Letters* **38**, doi:10.1029/2011gl048315 (2011).
- 715 88 Boyd, P. W. & Ellwood, M. J. The biogeochemical cycle of iron in the ocean. *Nature
716 Geoscience* **3**, 675-682, doi:10.1038/ngeo964 (2010).

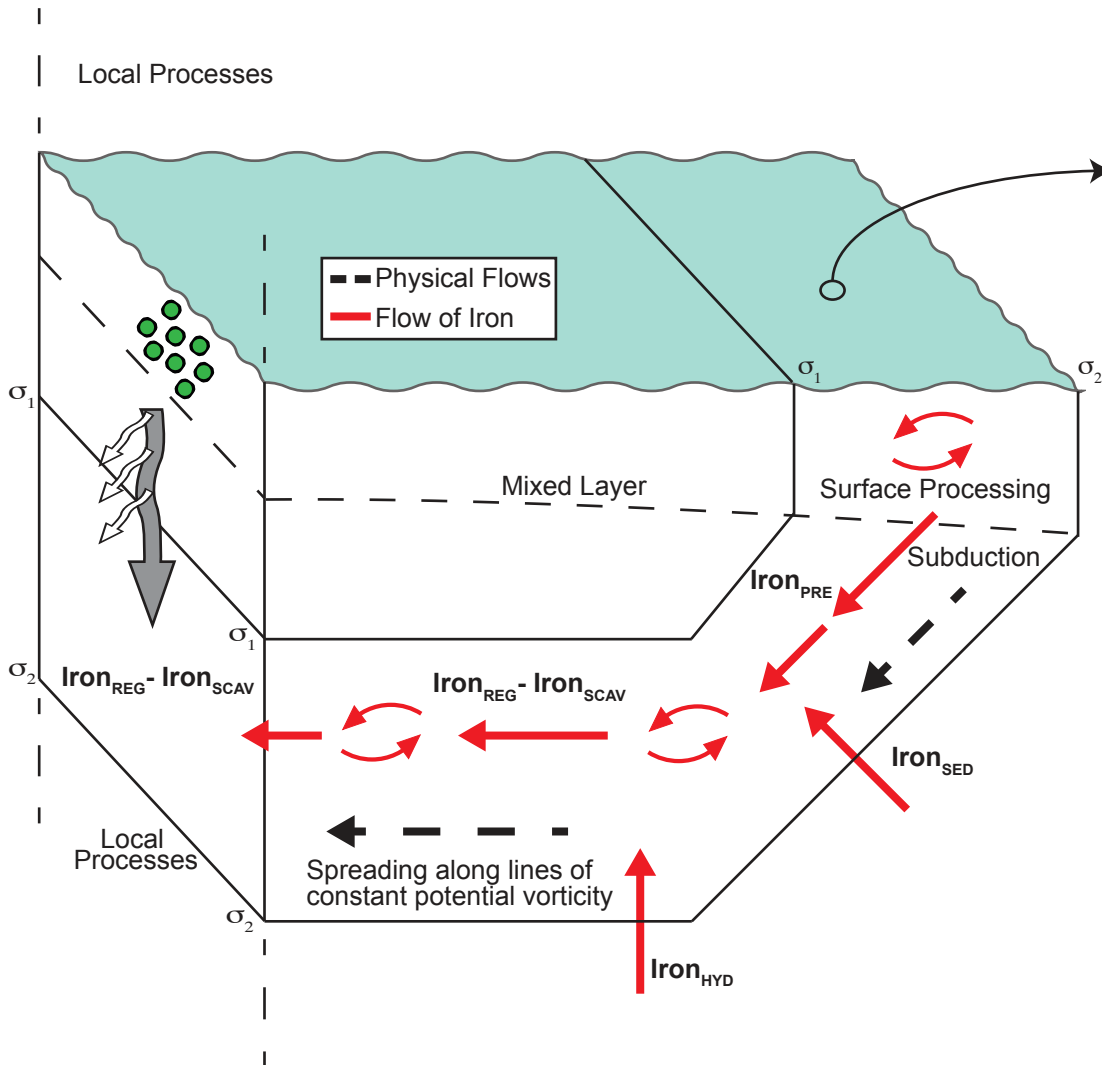
717 89 Lambert, F. *et al.* Dust fluxes and iron fertilization in Holocene and Last Glacial Maximum
718 climates. *Geophysical Research Letters* **42**, 6014-6023, doi:10.1002/2015gl064250 (2015).
719 90 Bopp, L. *et al.* Multiple stressors of ocean ecosystems in the 21st century: projections with
720 CMIP5 models. *Biogeosciences* **10**, 6225-6245, doi:10.5194/bg-10-6225-2013 (2013).
721 91 Keffer, T. The Ventilation of the World's Oceans: Maps of the Potential vorticity Field.
722 *Journal of Physical Oceanography* **15**, 509-523, doi:10.1175/1520-
723 0485(1985)015<0509:tvotwo>2.0.co;2 (1985).
724 92 Jenkins, W. J., Smethie, W. M., Boyle, E. A. & Cutter, G. A. Water mass analysis for the
725 U.S. GEOTRACES (GA03) North Atlantic sections. *Deep Sea Research Part II: Topical
726 Studies in Oceanography* **116**, 6-20, doi:10.1016/j.dsr2.2014.11.018 (2015).
727 93 Charette, M. A., Morris, P. J., Henderson, P. B. & Moore, W. S. Radium isotope
728 distributions during the US GEOTRACES North Atlantic cruises. *Marine Chemistry* **177**,
729 184-195, doi:10.1016/j.marchem.2015.01.001 (2015).
730 94 Wu, J., Boyle, E., Sunda, W. & Wen, L. S. Soluble and colloidal iron in the oligotrophic
731 North Atlantic and North Pacific. *Science* **293**, 847-849, doi:10.1126/science.1059251
732 (2001).
733 95 von der Heyden, B. P., Roychoudhury, A. N., Mtshali, T. N., Tyliszczak, T. & Myneni, S. C.
734 Chemically and geographically distinct solid-phase iron pools in the Southern Ocean.
735 *Science* **338**, 1199-1201, doi:10.1126/science.1227504 (2012).
736 96 Tortell, P. D., Maldonado, M. T. & Price, N. M. The role of heterotrophic bacteria in iron-
737 limited ocean ecosystems. *Nature* **383**, 330-332, doi:Doi 10.1038/383330a0 (1996).
738 97 Bonnain, C., Breitbart, M. & Buck, K. N. The Ferrojan Horse Hypothesis: Iron-Virus
739 Interactions in the Ocean. *Frontiers in Marine Science* **3**, doi:10.3389/fmars.2016.00082
740 (2016).
741 98 Mackey, K. R. *et al.* Divergent responses of Atlantic coastal and oceanic *Synechococcus* to
742 iron limitation. *Proceedings of the National Academy of Sciences of the United States of
743 America* **112**, 9944-9949, doi:10.1073/pnas.1509448112 (2015).
744 99 Hogle, S. L., Barbeau, K. A. & Gledhill, M. Heme in the marine environment: from cells to
745 the iron cycle. *Metallomics* **6**, 1107-1120, doi:10.1039/c4mt00031e (2014).
746 100 Ito, T. & Follows, M. J. Preformed phosphate, soft tissue pump and atmospheric CO₂.
747 *Journal of Marine Research* **63**, 813-839, doi:10.1357/0022240054663231 (2005).
748 101 Broecker, W. S., Takahashi, T. & Takahashi, T. Sources and flow patterns of deep-ocean
749 waters as deduced from potential temperature, salinity, and initial phosphate concentration.
750 *Journal of Geophysical Research* **90**, 6925, doi:10.1029/JC090iC04p06925 (1985).
751







a) Physical Linkages in the Iron Cycle



b) What makes up the different iron pools?

